

# COSMO-CLM<sup>2</sup>: a new version of the COSMO-CLM model coupled to the Community Land Model

Edouard L. Davin · Reto Stöckli · Eric B. Jaeger ·  
Samuel Levis · Sonia I. Seneviratne

Received: 23 March 2010 / Accepted: 31 January 2011  
© Springer-Verlag 2011

**Abstract** This study presents an evaluation of a new biosphere-atmosphere Regional Climate Model. COSMO-CLM<sup>2</sup> results from the coupling between the non-hydrostatic atmospheric model COSMO-CLM version 4.0 and the Community Land Model version 3.5 (CLM3.5). In this coupling, CLM3.5 replaces a simpler land surface parameterization (TERRA\_ML) used in the standard COSMO-CLM. Compared to TERRA\_ML, CLM3.5 comprises a more complete representation of land surface processes including hydrology, biogeophysics, biogeochemistry and vegetation dynamics. Historical climate simulations over Europe with COSMO-CLM and with the new COSMO-CLM<sup>2</sup> are evaluated against various data products. The simulated climate is found to be substantially affected by the coupling with CLM3.5, particularly in summer. Radiation fluxes as well as turbulent fluxes at the surface are found to be more realistically represented in COSMO-CLM<sup>2</sup>. This subsequently leads to improvements of several aspects of the simulated climate (cloud cover, surface temperature and precipitation). We show that a better partitioning of turbulent fluxes is the central factor

allowing for the better performances of COSMO-CLM<sup>2</sup> over COSMO-CLM. Despite these improvements, some model deficiencies still remain, most notably a substantial underestimation of surface net shortwave radiation. Overall, these results highlight the importance of land surface processes in shaping the European climate and the benefit of using an advanced land surface model for regional climate simulations.

**Keywords** Regional Climate Models · Land Surface Models · Land-atmosphere interactions · European climate

## 1 Introduction

Information about the regional characteristics of climate change is essential in order to quantify its impacts on human societies and ecosystems. To date, a large part of this regional information is derived from General Circulation Models (GCMs) (Christensen et al. 2007a). However, GCMs are still limited by their horizontal resolution, which is currently of the order of 200 km. At this rather coarse resolution, phenomena such as extreme weather events are not adequately resolved despite their strong relevance for impact assessments. Moreover, the effect of local forcings such as orography, coastlines and land cover can not be represented with sufficient details. To circumvent these problems, Regional Climate Models (RCMs) have been increasingly developed during the last two decades (Giorgi 2006). These RCMs are used to downscale large-scale information from GCMs at finer resolutions.

Historically, RCM development has been to a large extent inspired by (or directly based on) preexisting Numerical Weather Prediction (NWP) systems. While slow

---

E. L. Davin (✉) · R. Stöckli · E. B. Jaeger · S. I. Seneviratne  
Institute for Atmospheric and Climate Science, ETH Zurich,  
Zurich, Switzerland  
e-mail: edouard.davin@env.ethz.ch

S. I. Seneviratne  
e-mail: sonia.seneviratne@env.ethz.ch

*Present Address:*  
R. Stöckli  
Climate Services, Climate Analysis, MeteoSwiss,  
Zurich, Switzerland

S. Levis  
Climate and Global Dynamics Division, National Center for  
Atmospheric Research, Boulder, CO, USA

processes (e.g., ocean, sea ice and land dynamics) may be negligible in the context of NWP, they have to be taken into account for climate applications. For this reason, an important on-going activity in the area of RCM development is the coupling of the atmospheric component with other components of the climate system (ocean, sea ice, glaciers, biosphere, atmospheric chemistry, etc...).

In particular, the coupling with comprehensive Land Surface Models (LSMs) constitutes a major aspect of RCM development. Land surface processes can indeed affect climate in various ways such as through biogeophysical processes (Bonan 2008; Seneviratne et al. 2010) or biogeochemical feedbacks (Arneth et al. 2010). Already at an early stage of regional model development, the key role of land-atmosphere interactions has been recognized (see e.g., Pielke et al. 1998 for a review). For example, Avissar and Pielke (1989) implemented a parameterization of subgrid scale surface heterogeneity in a mesoscale model and found an impact on local circulations where contrasts in sensible heating were generated by surface heterogeneity. It was further demonstrated that mesoscale atmospheric circulations can be strongly influenced by the parameterization of stomatal conductance, due to its strong control on the Bowen ratio (Avissar and Pielke 1991). More recently, Lu et al. (2001) coupled the RAMS (Regional Atmospheric Modelling System) model to the CENTURY biogeochemistry model and showed that seasonal vegetation phenological variations significantly influence regional climate owing to their effect on water and energy exchanges. RAMS was also coupled to the SiB (Simple Biosphere) model (Denning et al. 2003) in order to simulate regional  $CO_2$  fluxes and atmospheric  $CO_2$  concentrations. SiB-RAMS was found to realistically reproduce diurnal and synoptical variations in  $CO_2$  fluxes and concentrations over North America (Denning et al. 2003; Wang et al. 2007). Steiner et al. (2009) replaced the Biosphere-Atmosphere Transfer Scheme (BATS) implemented in RegCM3 (Regional Climate Model version 3) by the more advanced Community Land Model version 3 (CLM3) and found substantial improvements in the simulated climate over West Africa. Specifically, the new version with CLM3 better simulates the timing of the monsoon advance and retreat across the Guinean Coast, and reduces precipitation and temperature biases. Overall, these studies demonstrated that a realistic description of land surface processes is necessary in order to correctly simulate regional climates.

In spite of the aforementioned efforts, most current RCMs still have relatively unsophisticated land surface parameterizations. For instance, most of the RCMs used in the PRUDENCE project (Christensen et al. 2007b; Jacob et al. 2007) and in the more recent ENSEMBLES project (Christensen et al. 2008) still include so-called 2nd

generation land surface schemes, although these relatively old schemes have been superseded by more advanced 3rd generation schemes. 3rd generation schemes include in particular a more process-based representation of evapotranspiration by explicitly resolving the process of photosynthesis and its control on stomatal conductance (see e.g., Sellers et al. 1997 and Pitman 2003, for an historical overview of LSM development).

In this study, we upgraded the land surface scheme of the COSMO-CLM regional model from its standard 2nd generation scheme to a more advanced 3rd generation scheme. The COSMO-CLM model is extensively used, especially over Europe, for both operational weather forecasting and regional climate modelling (e.g., Rockel et al. 2008; Anders and Rockel 2009; Hohenegger et al. 2009; Jaeger et al. 2009; Muhlbauer and Lohmann 2009; Lorenz et al. 2010; Zahn and von Storch 2010; Jaeger and Seneviratne in press; Kothe et al. in press). In its standard version COSMO-CLM includes a relatively simple land surface parameterization, which we replaced by the more comprehensive Community Land Model version 3.5 (CLM3.5). CLM3.5 comprises a mechanistic representation of the biogeophysical and biogeochemical processes that determine the exchanges of radiation, heat, water and carbon between the land and the atmosphere.

In the following, we evaluate these two versions of COSMO-CLM (sharing the same atmospheric scheme but using two different LSMs) over Europe. Specifically, we address the two following questions: (1) Is the European climate as simulated by COSMO-CLM sensitive to the representation of land surface processes? (2) Does a more comprehensive representation of these processes lead to a more realistic climate?

## 2 Methods

### 2.1 Model description

#### 2.1.1 COSMO-CLM

The Regional Climate Model COSMO-CLM is jointly developed by the Consortium for Small-scale Modelling (COSMO) and the Climate Limited-area Modelling Community (CLM-Community). These two groups, respectively encompassing European national weather services and climate research centers, unify their efforts in maintaining a common model for both operational weather prediction and regional climate simulations. In this study, we use COSMO-CLM version 4.0. This model version (along with an earlier version) has been extensively evaluated by Jaeger et al. (2008). In the following we summarize the main characteristics of the model. A fully

detailed technical documentation of the model is available at <http://www.cosmo-model.org>.

The COSMO-CLM dynamical core is based on the primitive thermodynamical equations describing atmospheric motions. A non-hydrostatic and fully compressible form of these equations is used, allowing applications on a wide range of spatial scales. The model equations are discretized on a three-dimensional grid based on a rotated geographical coordinate system. In the vertical, a generalized terrain-following height coordinate is used. The time integration is performed using a second-order leapfrog scheme. The prognostic variables are the horizontal and vertical wind components, pressure perturbation, temperature, specific humidity, cloud water and ice content, Turbulent Kinetic Energy (TKE) and specific water content of rain and snow.

COSMO-CLM comprises a set of physical parameterizations representing various processes. The vertical radiative fluxes within the atmosphere are calculated based on a so-called  $\delta$ -two-stream solution of the radiative transfer equation, using 3 spectral intervals in the solar part and 5 spectral intervals in the thermal part of the spectrum (Ritter and Geleyn 1992). The radiatively active constituents are water vapour, cloud water, cloud ice, ozone, aerosols, carbon dioxide and other minor trace gases. Vertical turbulent mixing is parameterized according to a level 2.5 closure using TKE as a prognostic variable (Mellor and Yamada 1974, 1982). For moist convection the mass flux scheme of Tiedtke (1989) is used, with equilibrium closure based on moisture convergence. The formation of grid-scale clouds and subsequent precipitation is parameterized by a bulk microphysics scheme including water vapour, cloud water, cloud ice, rain and snow. Subgrid-scale cloudiness is interpreted by an empirical function

depending on relative humidity and height. A corresponding cloud water content is also interpreted.

### 2.1.2 TERRA\_ML

Land surface processes are parameterized in the standard COSMO-CLM through the soil module TERRA\_ML (Grasselt et al. 2008, and references therein). The ultimate goal of any land surface parameterization is the provision of the lower boundary conditions to the atmospheric model in the form of surface fluxes of energy and mass. In COSMO-CLM these fluxes are calculated in the atmospheric part of the code, based on a stability and roughness length dependent flux formulation. However, their calculation requires the knowledge of surface temperature and surface specific humidity. The task of TERRA\_ML is to predict these quantities, which is achieved by solving simultaneously the thermal and hydrological budgets of the soil. The multi-layer structure adopted for both thermal and hydrological calculations is described in Table 1. The vertical distribution of soil temperature is calculated by solving the heat conduction equation (Fourier's law). The upper boundary condition is obtained by computing the energy balance at the surface, while the lower boundary condition is given by a prescribed climatological temperature. The hydrological part of TERRA\_ML predicts soil water content by solving the Richards' equation. The water content of above-ground reservoirs such as snow and canopy interception is also predicted. The source of water from the atmosphere is through precipitation, dew and rime. The sink terms are runoff and evapotranspiration, the representation of which is based on the BATS model (Dickinson 1984).

**Table 1** Multi-layer structure of the soil column in TERRA\_ML versus CLM3.5

|  | TERRA_ML  | CLM3.5   |
|--|---|--|
| Total number of layers   | 10  | 10   |
| Same layer structure for thermal and hydrological calculations | Yes   | Yes  |
| Depth of deepest layer (at bottom) (m)                         | 15.24   | 3.43   |
| Number of thermally active layers                              | 9   | 10   |
| Depth of last thermally active layer (at bottom) (m)           | 7.76  | 3.43   |
| Concept of thermal calculation                                 | Heat conduction equation                          | Heat conduction equation   |
| Type of bottom boundary condition for thermal part             | Constant climatological temperature in last layer | Zero heat flux condition   |
| Number of hydrologically active layers                         | 7   | 10   |
| Depth of last hydrologically active layer (at bottom) (m)      | 2   | 3.43   |
| Concept of hydrological calculation                            | Richards' equation                                | Richards' equation   |
| Type of bottom boundary condition for hydrological part        | Only gravitational drainage                       | Coupled with underlying aquifer, or zero-flux condition if the water table is within the soil column |

### 2.1.3 CLM3.5

To improve the representation of land surface processes in COSMO-CLM, we implemented a new model version (referred to as COSMO-CLM<sup>2</sup>) in which the TERRA\_ML module is replaced by the more comprehensive (3rd generation) Community Land Model version 3.5 (CLM3.5) maintained at the National Center for Atmospheric Research (NCAR). CLM3.5 is a state-of-the-art Land Surface Scheme representing land surface processes in the context of climate simulations. It is the land component of the Community Climate System Model (CCSM) (Collins et al. 2006; Dickinson et al. 2006) and earlier versions of CLM3.5 have also been coupled to other regional climate models (Steiner et al. 2005, 2009; Kumar et al. 2008). Biogeophysical processes represented by CLM3.5 include radiation interactions with vegetation and soil, momentum and heat fluxes from vegetation and soil, heat transfer in soil and snow, soil, snow and canopy hydrology and stomatal physiology and photosynthesis. A full description of the model is provided in Oleson et al. (2004, 2008). Surface fluxes in CLM3.5 have been evaluated at specific sites (Stoeckli et al. 2008), while the large-scale hydrology has been evaluated by Oleson et al. (2008). Optionally, CLM3.5 also simulates biogeochemical and biogeographical processes such as carbon and nitrogen dynamics (Thornton et al. 2007), biogenic emissions (Levis et al. 2003; Heald et al. 2008) and ecosystem dynamics (Bonan and Levis 2006). In the present study, however, these biogeochemical and biogeographical processes are not considered.

### 2.1.4 Differences between TERRA\_ML and CLM3.5

The representation of land processes differs considerably between CLM3.5 and TERRA\_ML. A summary of these differences is given here.

**2.1.4.1 Surface heterogeneity** In TERRA\_ML, the sub-grid-scale heterogeneity of the land surface is not explicitly accounted for (beside considering the partial coverage of the soil surface by vegetation and snow for albedo and evapotranspiration calculations). Only one soil column can exist in each grid cell (ice, rock or one out of 6 predefined soil types). If the grid cell is not ice or rock, vegetation can be present and is characterized by a grid average Leaf Area Index (LAI) and root depth, without further distinction between different plant types. On the other hand, CLM3.5 explicitly represents the subgrid-scale variability of the land surface using a tile approach. Each grid cell is decomposed into multiple land units (e.g., glacier, lake, vegetated surface, etc), soil/snow columns and Plant Functional Types (PFTs) (Oleson et al. 2004). Surface

fluxes are calculated at the PFT subgrid level. By default 4 (though this number is flexible) out of 15 possible PFTs that differ in physiology and structure can coexist on a single column. These 15 PFTs are meant to capture the differences between broad categories of plants by grouping plant species with similar biogeophysical and biogeochemical characteristics. Bare soil can be assigned to one of these 4 tiles instead of a PFT.

**2.1.4.2 Radiation fluxes** In the case of TERRA\_ML, upward fluxes of solar and infrared radiation are derived from a simulated grid-scale surface albedo and temperature, respectively. In CLM3.5, the treatment of radiation fluxes is far more complex. The shortwave and longwave radiation fluxes are calculated for both the canopy layer and the soil/snow surface using the two-stream approximation of the radiative transfer equation (Oleson et al. 2004). Explicit treatment of diffuse versus direct solar radiation is included. The canopy is divided into sunlit (receiving both direct and diffuse light) and shaded (receiving only diffuse light) fractions (Thornton and Zimmermann 2007).

**2.1.4.3 Turbulent fluxes** Surface turbulent fluxes are calculated in CLM3.5 using the Monin–Obukhov similarity theory (Oleson et al. 2004). In TERRA\_ML, the surface fluxes parameterization is intimately connected with the TKE-based turbulent mixing scheme (see Sect. 2.1.1). The dimensionless coefficients in the surface-layer Monin–Obukhov stability functions are expressed through the dimensionless coefficients of the Mellor–Yamada closure. In the case of CLM3.5, the sensible and latent heat are partitioned into vegetation and ground fluxes that depend on vegetation and ground temperatures.

**2.1.4.4 Hydrology** In both models, the Richards' equation is solved numerically for a multi-layer column to determine the vertical distribution of soil moisture (see Table 1 for a comparison of the multi-layer structure adopted in TERRA\_ML and CLM3.5). CLM3.5 comprises several hydrological extensions compared to TERRA\_ML. One relates to the lower boundary condition: whereas only downward gravitational drainage is assumed in TERRA\_ML below the last active soil layer, CLM3.5 features a prognostic groundwater model (Niu et al. 2007). This enables a dynamic coupling between the soil column and the underlying aquifer and to represent cases where the water table lies below the actual soil column. Surface and subsurface runoff representation in CLM3.5 is based on a TOPMODEL approach (Beven et al. 1984) adapted for the purpose of global climate simulations (Niu et al. 2005). The main principle of this approach is first the determination of a water table level based on the soil moisture state

and then the saturated fraction of the grid cell based on topographic characteristics. Surface runoff is then calculated as a combination of two processes: runoff over saturated ground and infiltration excess. Subsurface runoff is calculated as an exponential function of the water table depth. On the other hand, TERRA\_ML uses a simple formula for surface runoff (Hillel 1980) and determines subsurface runoff for each layer as the water amount exceeding the field capacity. Finally, the treatment of snow is relatively simple in TERRA\_ML. The water content of snow is determined by a single mass balance equation. The snow depth and snow density are also calculated for snow temperature prediction. A more comprehensive snow model is implemented in CLM3.5. This model predicts both the mass of ice and the mass of liquid water inside the snow pack, which is divided into as many as 5 layers. The processes represented include snow accumulation and compaction, melt-freeze cycle and water transfer between snow layers.

**2.1.4.5 Stomatal conductance and photosynthesis** Stomatal conductance, which represents the stomatal control on water transfer by plants, plays an important role in the calculation of evapotranspiration (ET). In TERRA\_ML stomatal conductance is calculated as in Dickinson (1984) based on an empirical relationship correlating stomatal conductance to environmental factors (light, soil moisture, temperature and atmospheric humidity). This approach, corresponding to the second generation of LSMs (Sellers et al. 1997), does not represent the process of photosynthesis which is the actual mechanism controlling stomatal functioning. The third generation of LSMs, to which CLM3.5 belongs, introduces explicitly a link between stomatal conductance and photosynthetic activity (Sellers et al. 1997). In CLM3.5, the formulation of stomatal conductance is adapted from Collatz et al. (1991). The calculation of photosynthetic assimilation distinguishes C3 and C4 metabolic pathways. Leaf photosynthesis is computed after Farquhar et al. (1980) and Collatz et al. (1991) for C3 plants and after Collatz et al. (1992) and Dougherty et al. (1994) for C4 plants.

**2.1.4.6 Surface datasets** Both CLM3.5 and TERRA\_ML require input datasets specifying land surface characteristics, such as land cover, vegetation parameters and soil texture. The surface input datasets used in CLM3.5 are fully described in Lawrence and Chase (2007), while a description of TERRA\_ML input datasets is provided by Smiatek et al. (2008). CLM3.5 uses land cover, LAI, and soil color maps derived from MODIS satellite products. In TERRA\_ML, the Global Land Cover map for the year 2000 (GLC2000) developed by the Joint Research Center of the European Commission (JRC) is used to determine vegetation parameters such as LAI and root depth. These

parameters are derived from the land cover map by application of look-up tables and calculation of the grid average. Soil texture in TERRA\_ML is derived from the Food and Agriculture Organization of the United Nations (FAO) Digital Soil Map of the World. The FAO soil map provides soil texture information for the top soil layer (0–30 cm) and the bottom soil layer (30–100 cm). TERRA\_ML uses only the top layer information across all model layers. In contrast, CLM3.5 takes into account the vertical heterogeneity of soil texture. The International Geosphere-Biosphere Programme (IGBP) soil dataset (Global Soil Data Task 2000) of 4,931 soil mapping units and their sand and clay content for each soil layer were used to create a soil texture dataset that varies with depth (Bonan et al. 2002).

## 2.2 Experiments

Two climate simulations are analysed in this study. The first experiment is a control simulation with the standard COSMO-CLM model. (Note that this experiment is the same as the one analyzed by Jaeger et al. (2008) and referred to as CCLM-44 therein.) The second experiment is performed with COSMO-CLM<sup>2</sup>, the version of COSMO-CLM coupled to CLM3.5.

Both experiments use a horizontal resolution of 0.44° (~50 km) with 32 atmospheric levels in the vertical and a time step of 240s. The model domain encompasses the entire European continent, including parts of northern Africa and of Russia. The simulations cover the period from 1980 to 2006. ERA40 reanalysis data (Uppala et al. 2005) are used as lateral boundary conditions, except for the years 2002–2006 where ECMWF operational forecast analyses are employed. Note that a similar set-up for boundary conditions has been used in previous studies (e.g., Jaeger et al. 2008; Lorenz et al. 2010; Jaeger and Seneviratne in press) and has not been shown to lead to discontinuities in the atmospheric forcing due to the consistency between the two products (Hirschi et al. 2006). CO<sub>2</sub>, CH<sub>4</sub> and N<sub>2</sub>O concentrations are prescribed according to observed historical trends. The first 6 years are used as spin-up time and only the following years (1986–2006) are analysed. Since the experimental setup and the atmospheric part of the model are identical in the two experiments, their comparison strictly isolates the effect of introducing a new land surface scheme in COSMO-CLM.

## 2.3 Evaluation datasets

Several datasets are employed in this study for model evaluation. For 2-m temperature, precipitation and total cloud cover, we use the Climate Research Unit (CRU) global 0.5° gridded dataset version CRU TS3.0 (Mitchell and Jones 2005).

We also use the International Satellite Cloud Climatology Project (ISCCP) D2 dataset at  $280 \times 280$  km resolution (Rossow and Schiffer 1999) as an alternative cloud cover dataset.

For precipitation, the Global Precipitation Climatology Project (GPCP) version 2.1 data set (Adler et al. 2003) is also employed. This global data set consists of monthly means of precipitation derived from satellite and gauge measurements. Although the GPCP product has a relatively coarse resolution ( $2.5^\circ$ ), it presents the advantage of including a correction to compensate for systematic biases in gauge measurements due to wind, gauge wetting and gauge evaporation. Since the CRU data set doesn't include such correction, the complementary use of the GPCP product can help identifying the effect of systematic errors in precipitation measurements in our comparisons.

To evaluate surface fluxes, we use the global  $1^\circ$  gridded dataset from the Global Soil Wetness Project (GSWP-2) (Dirmeyer et al. 2006). This product is based on 13 LSMs which were all driven by the same observationally-based meteorological forcing for the period 1986–1995. In this study, we consider the multi-model mean from the GSWP-2 dataset as well as the multi-model standard deviation. We used  $\pm 2 \times \text{SD}$  as an estimate of the uncertainty range of the GSWP-2 dataset.

To complement the GSWP-2 dataset, we also use observations of latent and sensible heat from the FLUXNET network (Baldocchi et al. 2001). We consider data from 10 different sites over Europe, whose characteristics are summarized in Table 2. These same sites have already been considered in an evaluation of an earlier version of COSMO-CLM (Jaeger et al. 2009). The selection of these stations is based on maximum spatial and temporal data coverage across Europe. As in Jaeger et al. (2009), the data were not gap-filled and comparison to the model output is only done at times when no gaps occur. Random measurement errors in turbulent fluxes are estimated based

on empirical relationships derived by Richardson et al. (2006).

We applied no corrections (e.g., height correction) to the various datasets. For comparison with model results, we interpolated the model outputs onto the respective dataset grids. In the case of the FLUXNET sites, we consider the model grid cell encompassing the site coordinates for comparison with observations. Jaeger et al. (2009) noted that taking a weighted value from several neighbouring grid cells as an alternative method does not lead to significant differences in such comparisons. For some analyses the results are aggregated over specific regions. For this we used the European sub-domains as defined in the PRUDENCE project (Christensen et al. 2007b).

### 3 Results

#### 3.1 Surface climate

Differences between model and observations for 2-meter temperature and precipitation are presented in Figs. 1 and 2, respectively. The comparison between the two model versions highlights the influence of the coupling with CLM3.5. Winter temperatures are reasonably well simulated in both model versions over most of Europe, except for a warm bias over Northern Scandinavia. Only minor differences between COSMO-CLM and COSMO-CLM<sup>2</sup> appear during this season. In summer, COSMO-CLM exhibits a very pronounced cold bias (above 2 K) north of  $45^\circ$ . This well known feature of COSMO-CLM version 4.0 has been attributed to an overestimation of cloud cover, consequently leading to an underestimation of short wave radiation at the surface (Jaeger et al. 2008). This cold bias is totally suppressed in COSMO-CLM<sup>2</sup>, which shows a very good agreement with observed temperature. Reasons for this result will be further investigated in the following sections.

**Table 2** Overview of the FLUXNET sites used in this study (from North to South)

| Site and reference                        | Short | Lon ( $^\circ\text{E}$ ) | Lat ( $^\circ\text{N}$ ) | Alt (m) | Biome type     | Period used |
|---|-------|--------------------------|--------------------------|---------|----------------|-------------|
| Kaamanen (Laurila et al. 2001)            | FIKaa | 27.30                    | 69.14                    | 155     | Wetland/Tundra | 2002–2005   |
| Sodankyla (Hatakka et al. 2003)           | FISod | 26.64                    | 67.36                    | 180     | Evergreen      | 2002–2005   |
| Hyytiala (Suni et al. 2003)               | FIHyy | 24.29                    | 61.85                    | 181     | Evergreen      | 2002–2005   |
| Fyodorovskoye (Milyukova et al. 2002)     | RUFyo | 32.92                    | 56.46                    | 265     | Evergreen      | 2002–2005   |
| Vielsalm (Aubinet et al. 2001)            | BEVie | 6.00                     | 50.31                    | 450     | Mixed          | 2002–2005   |
| Bily Kriz Forest (Reichstein et al. 2005) | CZBK1 | 18.54                    | 49.50                    | 908     | Evergreen      | 2002–2005   |
| Sarrebourg (Granier et al. 2000)          | FRHes | 7.06                     | 48.67                    | 300     | Deciduous      | 2002–2005   |
| Renon (Marcolla et al. 2005)              | ITRen | 11.43                    | 46.59                    | 1,730   | Evergreen      | 2002–2005   |
| Puechabon (Reichstein et al. 2002)        | FRPue | 3.60                     | 43.74                    | 270     | Deciduous      | 2002–2005   |
| Amplero (Gilmanov et al. 2007)            | ITamp | 13.61                    | 41.90                    | 884     | Grassland      | 2002–2005   |

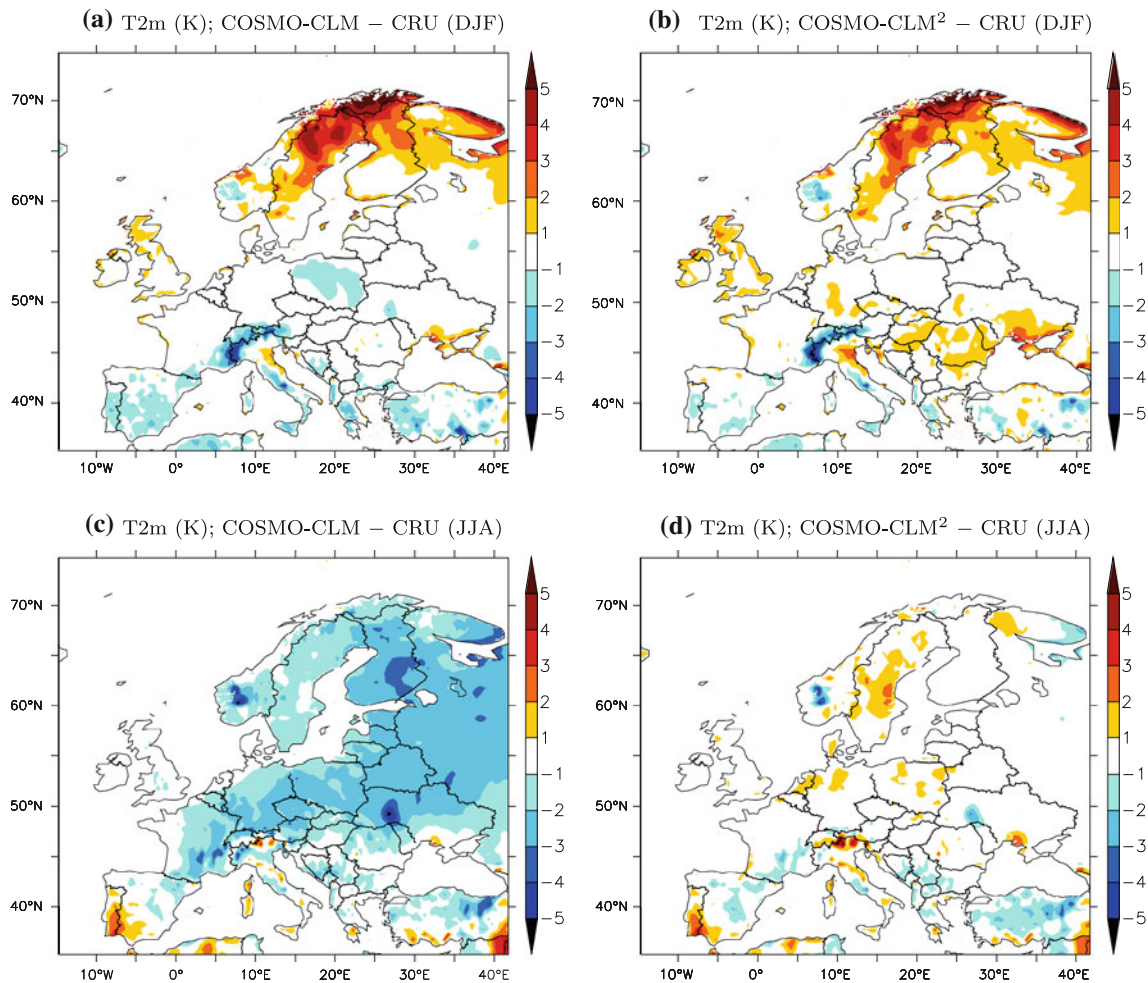


**Fig. 1** Mean 2-meter temperature bias for winter (**a** COSMO-CLM and **b** COSMO-CLM<sup>2</sup>) and for summer (**c** COSMO-CLM and **d** COSMO-CLM<sup>2</sup>). Biases are calculated in reference to the CRU dataset for the period 1986–1995

Examination of the precipitation biases (Fig. 2) indicates a strong overestimation of modeled precipitation in winter. In summer, biases are overall less pronounced, with rainfall being overestimated over northern Europe and underestimated over the Balkan Peninsula. Although these features occur in the two model versions, the coupling with CLM3.5 has a positive effect by slightly reducing the magnitude of the wet bias present over most regions in winter and over northern Europe in summer.

Figure 3 shows the seasonal cycle of precipitation for three different regions spanning a broad range of climates (Iberian Peninsula, Mid-Europe and Scandinavia). In addition to the CRU observations, the simulations are also compared to the GPCP dataset. As mentioned in Sect. 2.3, the GPCP product notably includes a correction to compensate for systematic underestimation of precipitation from gauge measurements. As a result, the precipitation values in GPCP are always higher than in CRU for the three regions in Fig. 3, particularly in winter. This suggests that part of the model overestimation of precipitation can

be explained by measurement errors rather than by model deficiencies. Over Mid-Europe, the agreement between GPCP and COSMO-CLM<sup>2</sup> is indeed very good, improving the general tendency of COSMO-CLM to overestimate precipitation. For Scandinavia, both model versions appear to overestimate precipitation over the whole year even in comparison to GPCP, with however a clear improvement in COSMO-CLM<sup>2</sup>. Over the Iberian Peninsula, the simulations are in good agreement with observations and the differences between the two model versions are very small.

Table 3 summarizes the influence of the coupling for every season as indicated by the root mean square error (RMSE) between model and observations. RMSEs are calculated spatially over the entire European domain for each season and are within 1–2 K for temperature and within 0.5–1.2 mm/day for precipitation. The coupling with CLM3.5 consistently reduces the magnitude of the errors for both temperature and precipitation in all seasons (except for temperature in autumn and winter where COSMO-CLM and COSMO-CLM<sup>2</sup> have similar

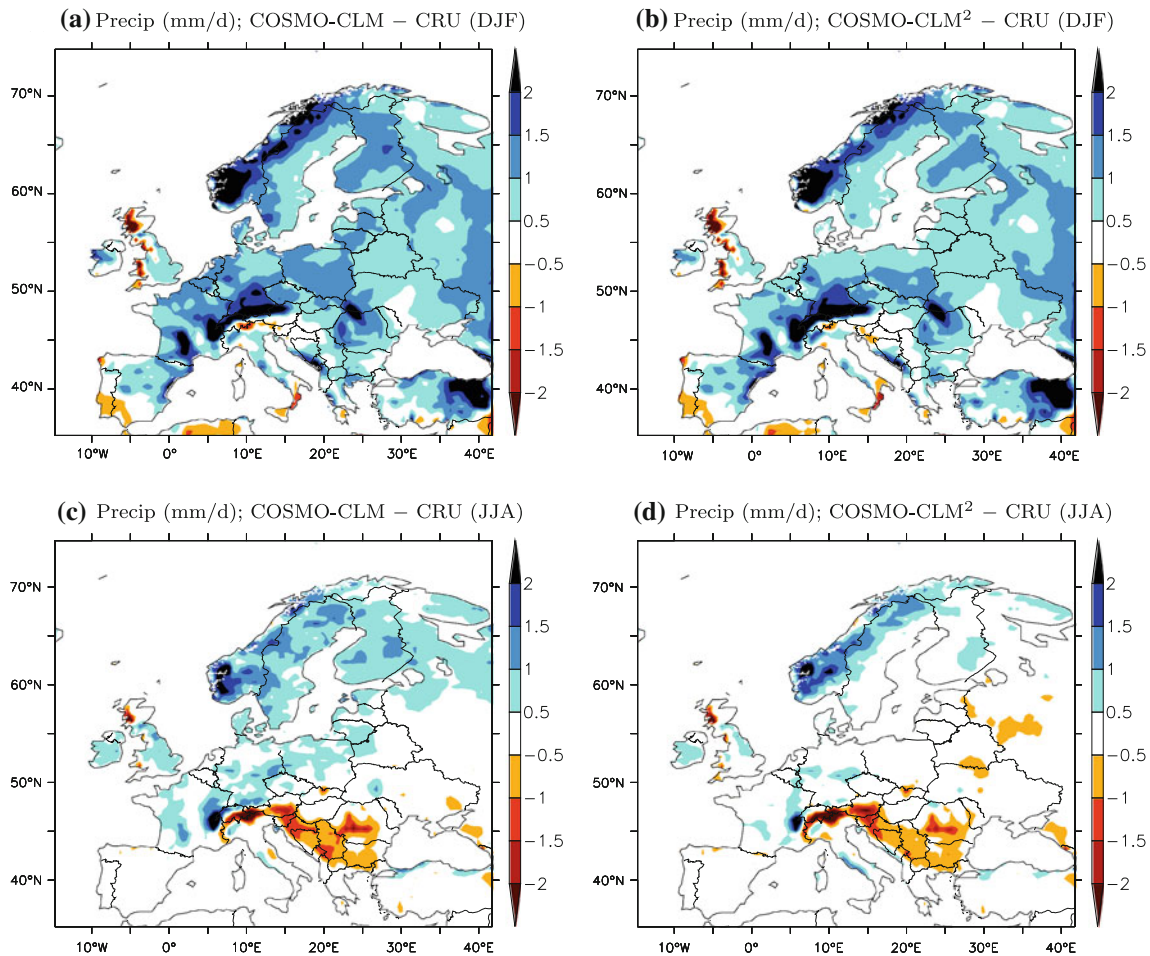


**Fig. 2** Mean precipitation bias for winter (**a** COSMO-CLM and **b** COSMO-CLM<sup>2</sup>) and for summer (**c** COSMO-CLM and **d** COSMO-CLM<sup>2</sup>). Biases are calculated in reference to the CRU dataset for the period 1986–1995

performances). Furthermore, the effect of the coupling appears to be stronger in spring and summer, where RMSE values differ much more between the two model versions. This can be interpreted as a consequence of the seasonally varying influence of land surface fluxes on climate. Surface fluxes are stronger and thus have a larger potential to affect atmospheric conditions during the warm season, whereas during the cold season atmospheric circulation is expected to have more influence on surface conditions.

The effect of the coupling being more prominent during the warm season, we focus mainly on summer in the following sections.

### 3.2 Radiation and clouds

Net radiation fluxes at the surface (positive downward) are presented in Fig. 4 as the difference between model and GSWP-2 data. As already reported by Jaeger et al. (2008), COSMO-CLM overestimates longwave net radiation and underestimates shortwave net radiation in summer. The

underestimation of net shortwave radiation is so pronounced that it largely offsets the longwave radiation bias. Therefore, total net radiation (bottom panel) is substantially underestimated in COSMO-CLM, over most parts of Europe. On the other hand, radiation fluxes are better simulated by COSMO-CLM<sup>2</sup>, both for longwave and shortwave radiation. The underestimation of net shortwave radiation and subsequently of total net radiation is still present in COSMO-CLM<sup>2</sup>, but is substantially reduced compared to COSMO-CLM.

We note that these biases are clearly above the uncertainty range of the GSWP-2 dataset, as indicated by the shading in Fig. 4. Moreover, we find similar biases when comparing the simulated radiation fluxes with the ERA40 reanalysis (not shown), thus indicating the robustness of these results.

For all radiation components, model biases strongly increase with latitude (Table 4). Over Scandinavia, the underestimation of net radiation in COSMO-CLM represents about 40% of the absolute GSWP-2 estimate. This is

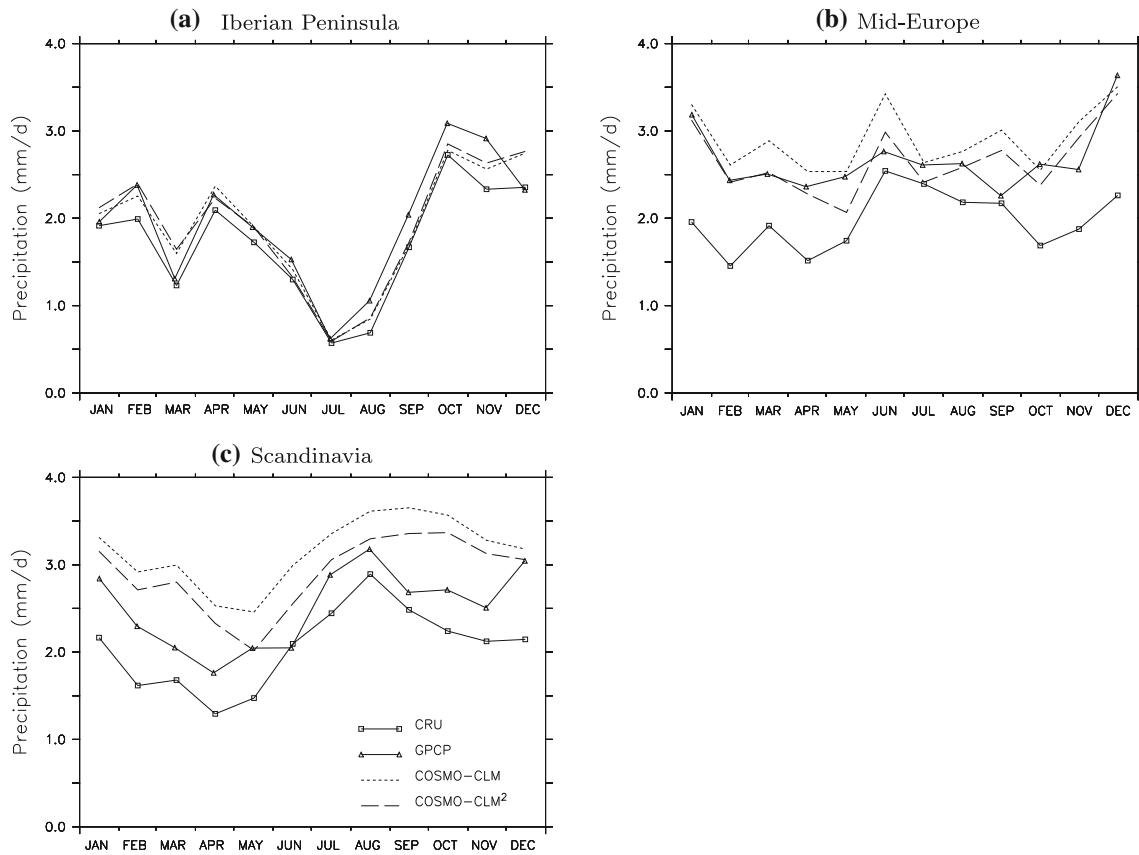


**Fig. 3** Mean seasonal cycle of precipitation over **a** the Iberian Peninsula, **b** Mid-Europe and **c** Scandinavia. Climatological means for CRU (squares), GPCP (triangles), COSMO-CLM (dotted line) and COSMO-CLM<sup>2</sup> (dashed line) are calculated for the period 1986–1995

**Table 3** Spatial RMSE for model versus CRU observations calculated for the entire European domain

|                        | t2m (K) |     |     |     | Precipitation (mm/day) |     |     |     |
|------------------------|---------|-----|-----|-----|------------------------|-----|-----|-----|
|                        | DJF     | MAM | JJA | SON | DJF                    | MAM | JJA | SON |
| COSMO-CLM              | 1.7     | 1.4 | 1.9 | 1.0 | 1.2                    | 1.0 | 0.7 | 1.0 |
| COSMO-CLM <sup>2</sup> | 1.7     | 1.0 | 1.0 | 1.0 | 1.1                    | 0.8 | 0.5 | 0.9 |

substantially decreased to 30% in COSMO-CLM<sup>2</sup>. For the Iberian Peninsula, the net radiation bias is the order of 10% in both versions, indicating a low sensitivity to the change in LSM over Southern Europe.

These deficiencies affecting the amount of radiation absorbed by the surface can be linked to the simulation of clouds. Figure 5 shows a comparison between model and observations for total cloud cover. Total cloud cover is strongly overestimated in COSMO-CLM with a spatial pattern in line with the radiation bias. Excess cloud cover increases the simulated downwelling atmospheric longwave radiation (Fig. 4a), but not as much as it reduces the downwelling shortwave radiation. As a result the net radiation is underestimated. COSMO-CLM<sup>2</sup> exhibits a

more realistic simulation of cloud cover (Fig. 5b, d), although the cloud overestimation is not fully corrected. This allows to partly alleviate the underestimation of surface net radiation.

There are important differences between the CRU and the ISCCP datasets. The magnitude of the bias is substantially smaller when comparing to ISCCP (Fig. 5c, d), but the sign of the bias remains consistent.

To interpret the model behaviour with respect to cloud cover, it is first necessary to analyse the changes in turbulent fluxes, which is done in the next section.

### 3.3 Turbulent fluxes

The radiative energy absorbed by the surface is to a large extent released to the atmosphere in the form of heat (sensible or latent) through turbulent fluxes. Because absorbed surface radiation is underestimated in both model versions (previous section), the total heat flux released to the atmosphere (sum of sensible and latent heat flux) is expected to be underestimated as well. The summer mean total heat flux, as simulated by the two model versions, is compared to the GSWP-2 multi-model mean in Fig. 6. As

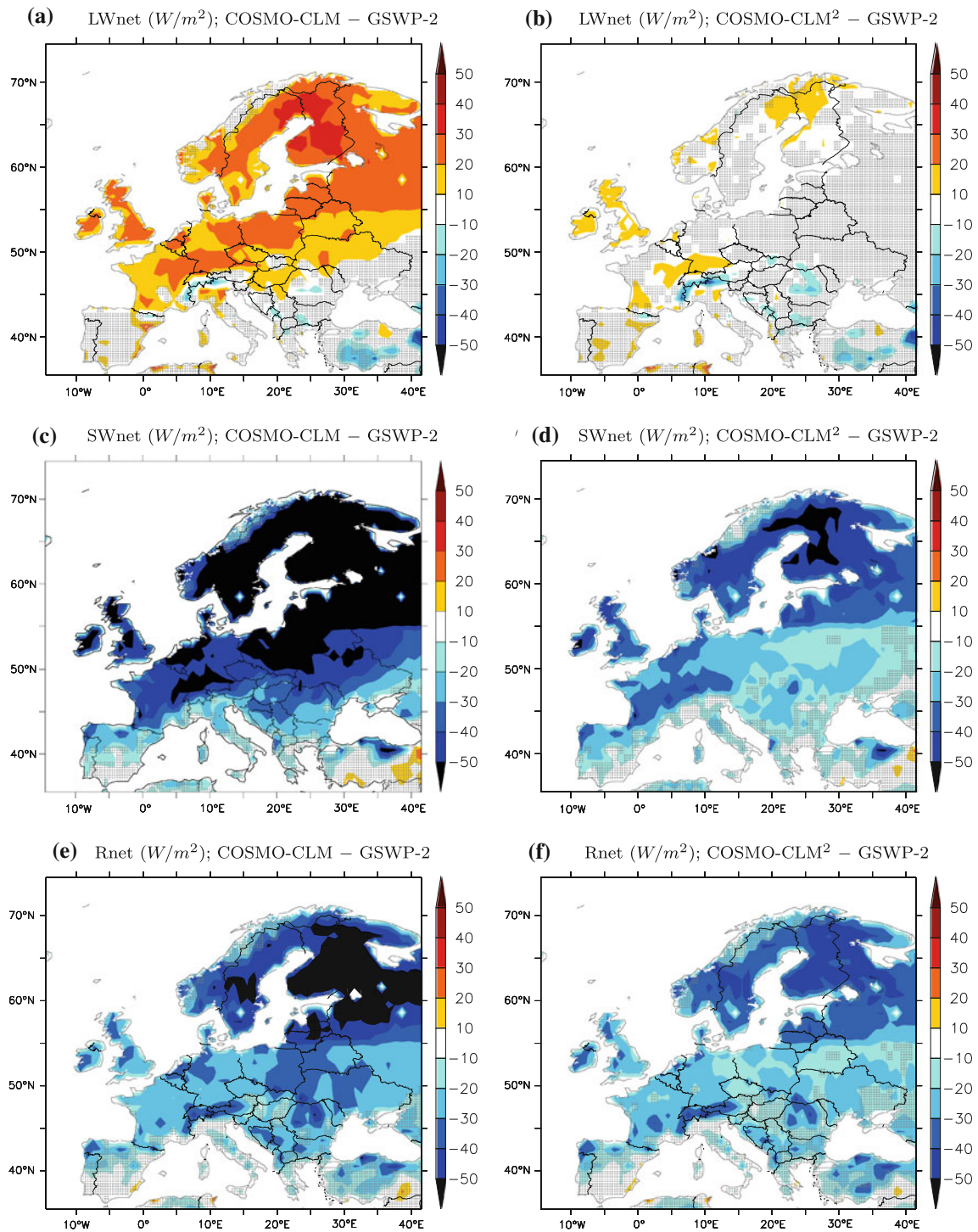


**Fig. 4** Summer (JJA) bias for surface net longwave radiation (**a** COSMO-CLM and **b** COSMO-CLM<sup>2</sup>), surface net shortwave radiation (**c** COSMO-CLM and **d** COSMO-CLM<sup>2</sup>) and surface net radiation (**e** COSMO-CLM and **f** COSMO-CLM<sup>2</sup>). Biases are

calculated in reference to the GSWP-2 multi-model mean for the period 1986–1995. Grey shading indicates that the model bias is within the GSWP-2 uncertainty range

expected, this quantity is underestimated in both model versions, although the underestimation is less pronounced in COSMO-CLM<sup>2</sup>, as it is also the case for absorbed surface radiation.

Since the absolute magnitude of the turbulent fluxes is directly affected by radiation biases (and thus does not reflect the intrinsic model skills in simulating these fluxes), it is more informative to analyse turbulent fluxes in terms

**Table 4** Comparison of the summer (JJA) radiation biases in COSMO-CLM and COSMO-CLM<sup>2</sup> over three selected regions

|                                 | Iberian Peninsula            |                              |                             | Mid-Europe                   |                              |                             | Scandinavia                  |                              |                             |
|---------------------------------|------------------------------|------------------------------|-----------------------------|------------------------------|------------------------------|-----------------------------|------------------------------|------------------------------|-----------------------------|
|                                 | LWnet<br>(W/m <sup>2</sup> ) | SWnet<br>(W/m <sup>2</sup> ) | Rnet<br>(W/m <sup>2</sup> ) | LWnet<br>(W/m <sup>2</sup> ) | SWnet<br>(W/m <sup>2</sup> ) | Rnet<br>(W/m <sup>2</sup> ) | LWnet<br>(W/m <sup>2</sup> ) | SWnet<br>(W/m <sup>2</sup> ) | Rnet<br>(W/m <sup>2</sup> ) |
| GSWP-2                          | -84.2                        | 221.7                        | 137.4                       | -54.7                        | 164.4                        | 109.7                       | -50.0                        | 163.5                        | 113.5                       |
| COSMO-CLM – GSWP-2              | 5.9                          | -20.1                        | -14.1                       | 21.6                         | -49.4                        | -27.9                       | 22.7                         | -66.8                        | -44.0                       |
| COSMO-CLM <sup>2</sup> – GSWP-2 | 5.8                          | -19.5                        | -13.7                       | 7.6                          | -30.7                        | -23.1                       | 4.8                          | -39.5                        | -34.6                       |

Biases are calculated in reference to the GSWP-2 dataset for the period 1986–1995. *LWnet* surface net longwave radiation; *SWnet* surface net shortwave radiation; *Rnet* surface net radiation

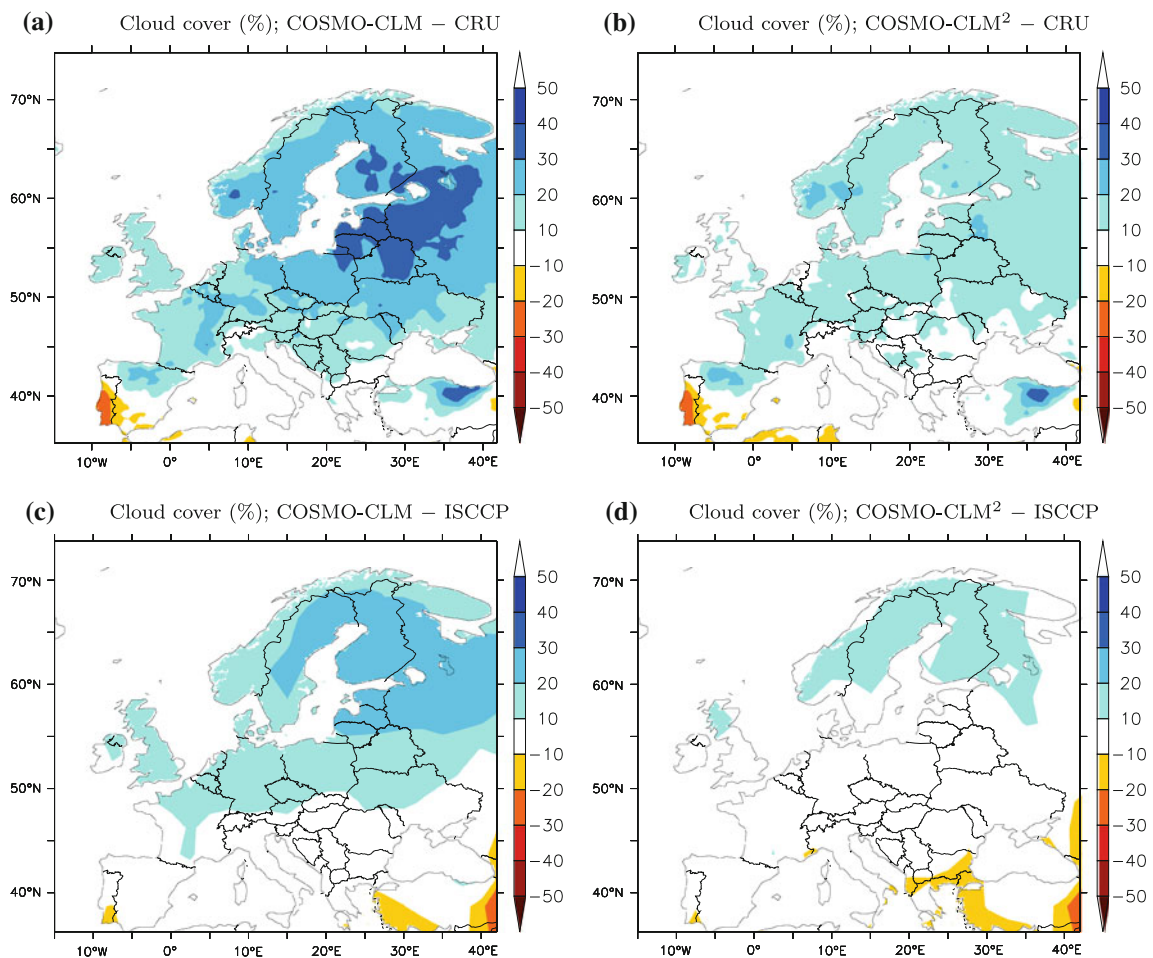


**Fig. 5** Summer (JJA) bias for cloud cover in reference to the CRU dataset (a and b) and in reference to the ISCCP dataset (c and d). Biases are calculated for the period 1986–1995

of their partitioning. We use the Bowen ratio ( $B$ ; sensible heat divided by latent heat) to address how the energy at the surface is partitioned into sensible and latent heat. Compared to the GSWP-2 multi-model mean (Fig. 6),  $B$  is too low in COSMO-CLM (too weak sensible heating compared to evapotranspiration). This bias is particularly

pronounced for the northern half of Europe, whereas the opposite behaviour can be seen over the Mediterranean area. Generally, latent heat flux is lower and sensible heat flux is higher in COSMO-CLM<sup>2</sup> compared to COSMO-CLM (not shown). Therefore,  $B$  in COSMO-CLM<sup>2</sup> is in better agreement with the GSWP-2 multi-model mean

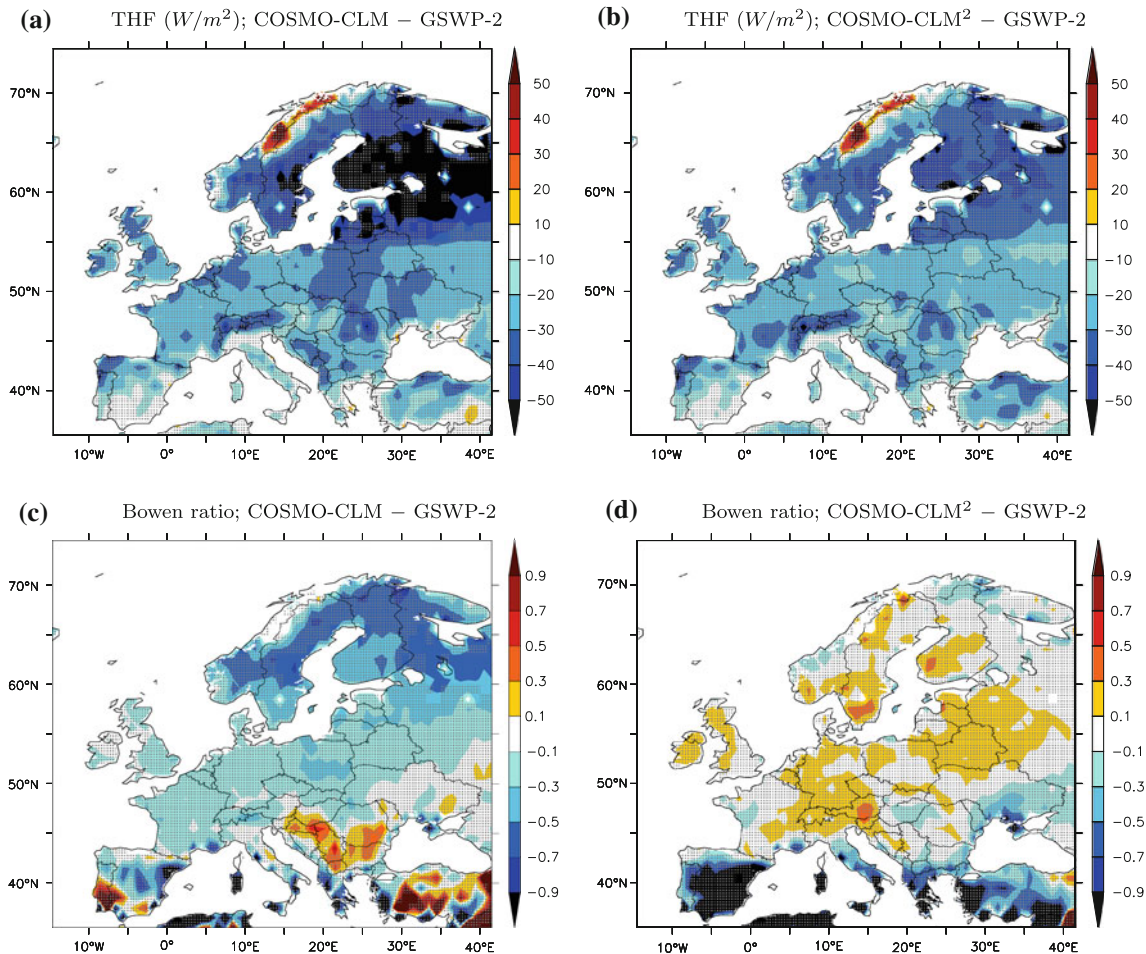


**Fig. 6** Summer (JJA) bias for total heat flux (THF: sum of sensible and latent heat fluxes) (a) COSMO-CLM and (b) COSMO-CLM<sup>2</sup> and for Bowen ratio (c) COSMO-CLM and (d) COSMO-CLM<sup>2</sup>. Biases are

calculated in reference to the GSWP-2 multi-model mean for the period 1986–1995. Grey shading indicates that the model bias is within the GSWP-2 uncertainty range

(Fig. 6), although its underestimation in COSMO-CLM seems to be slightly overcorrected for some regions in central Europe.

It is worthwhile to mention the large uncertainties associated with turbulent flux estimates. The grey shading in Fig. 6, indicating areas where model biases don't exceed the GSWP-2 uncertainty range, is present over most parts of Europe. Only COSMO-CLM has biases larger than the uncertainty range for some small regions over Northern Europe.

To complement these results, we also compare our simulations with flux measurements at different sites over Europe. Figure 7 shows the July mean diurnal cycle of  $B$  for 10 different sites. For all of these 10 sites,  $B$  as simulated by COSMO-CLM lies outside the uncertainty range of the measurements. In most cases COSMO-CLM underestimates  $B$ , which confirms the previous comparison with GSWP-2 data. COSMO-CLM<sup>2</sup> performs generally better: only 2 sites (Puechabon and Renon) show no improvements for COSMO-CLM<sup>2</sup> over COSMO-CLM, but

for the 8 other sites COSMO-CLM<sup>2</sup> is closer to observations. Furthermore, COSMO-CLM<sup>2</sup> lies within the uncertainty range of the measurements for the majority of the sites, thus substantially improving the initial performance of the standard COSMO-CLM.

### 3.4 Hydrology

The two LSMs strongly differ in their representation of land hydrology, which is reflected in the simulated soil moisture (Fig. 8a–c). Across different regions and seasons, COSMO-CLM<sup>2</sup> tends to simulate wetter soils than GSWP-2, whereas COSMO-CLM has drier soils than GSWP-2. However, both COSMO-CLM and COSMO-CLM<sup>2</sup> are within the GSWP-2 uncertainty range. We note that the differences in partitioning of surface fluxes described in the previous section can therefore not be related to differences in water availability. Indeed, COSMO-CLM<sup>2</sup> produces less evapotranspiration than COSMO-CLM despite having wetter soils.

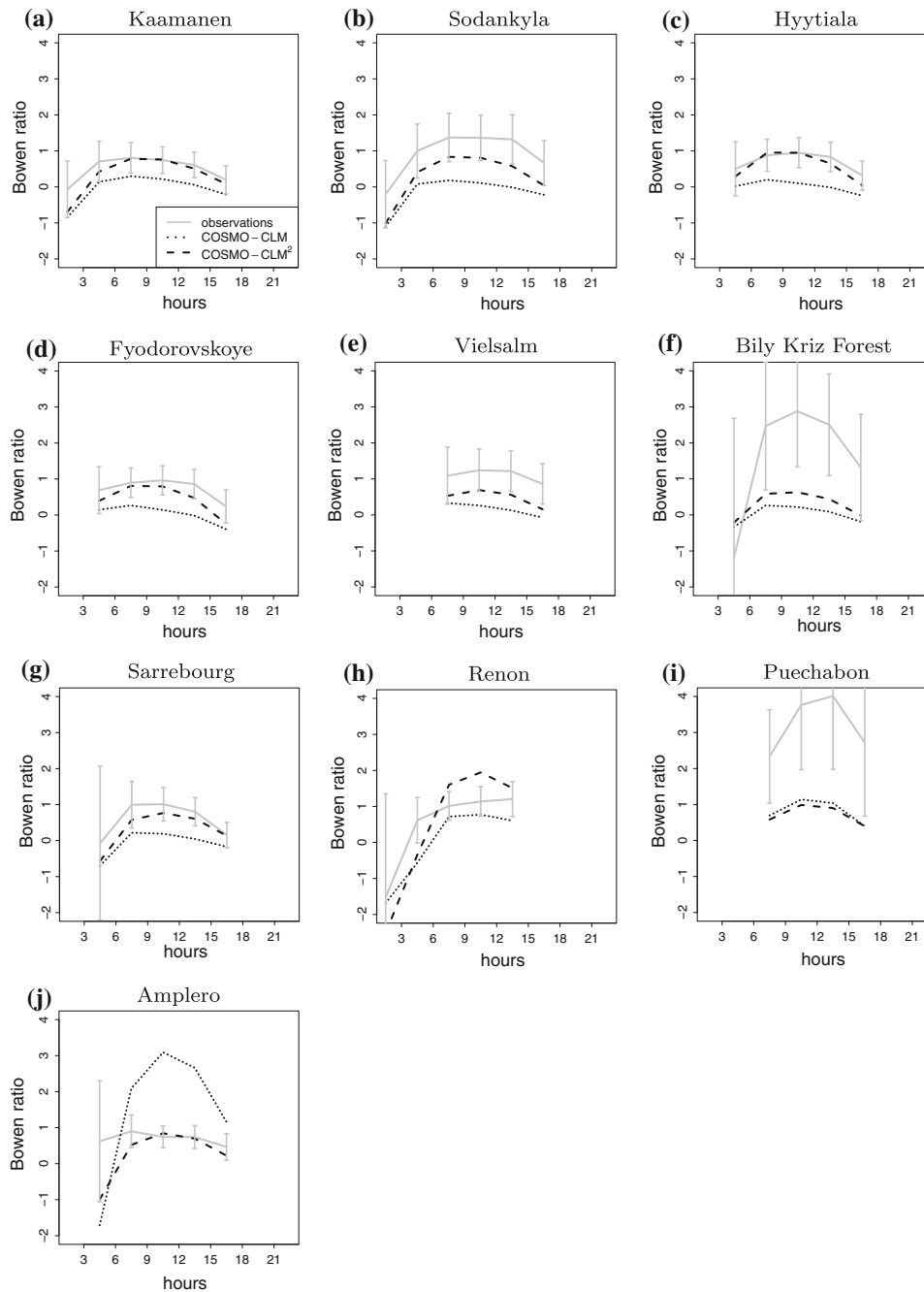


**Fig. 7** Mean diurnal cycle (July) of Bowen ratio at 10 different sites for FLUXNET measurements (*grey line*), COSMO-CLM (*dotted line*) and COSMO-CLM<sup>2</sup> (*dashed line*). Data are averaged over the period

2002–2005. The random measurement error is estimated based on an empirical method from Richardson et al. (2006)

The higher soil water content in COSMO-CLM<sup>2</sup> can not be related to the precipitation forcing, since precipitation is in general lower in COSMO-CLM<sup>2</sup> as compared to COSMO-CLM (Fig. 8d–f). Instead, this is due to the interaction between groundwater and the soil column in CLM3.5, a process not represented in TERRA\_ML. Because water from the underlying aquifer can recharge the soil column, soils tend to be wetter in CLM3.5.

The proportion of surface versus subsurface runoff is relatively similar in both models. The main difference occurs over Scandinavia during the runoff peak associated with the snowmelt season. In COSMO-CLM most of the snowmelt is lost through surface runoff (as infiltration is prevented by frozen soils), whereas in COSMO-CLM<sup>2</sup> the water from snowmelt infiltrates in the soil and thus increases subsurface more than surface runoff.

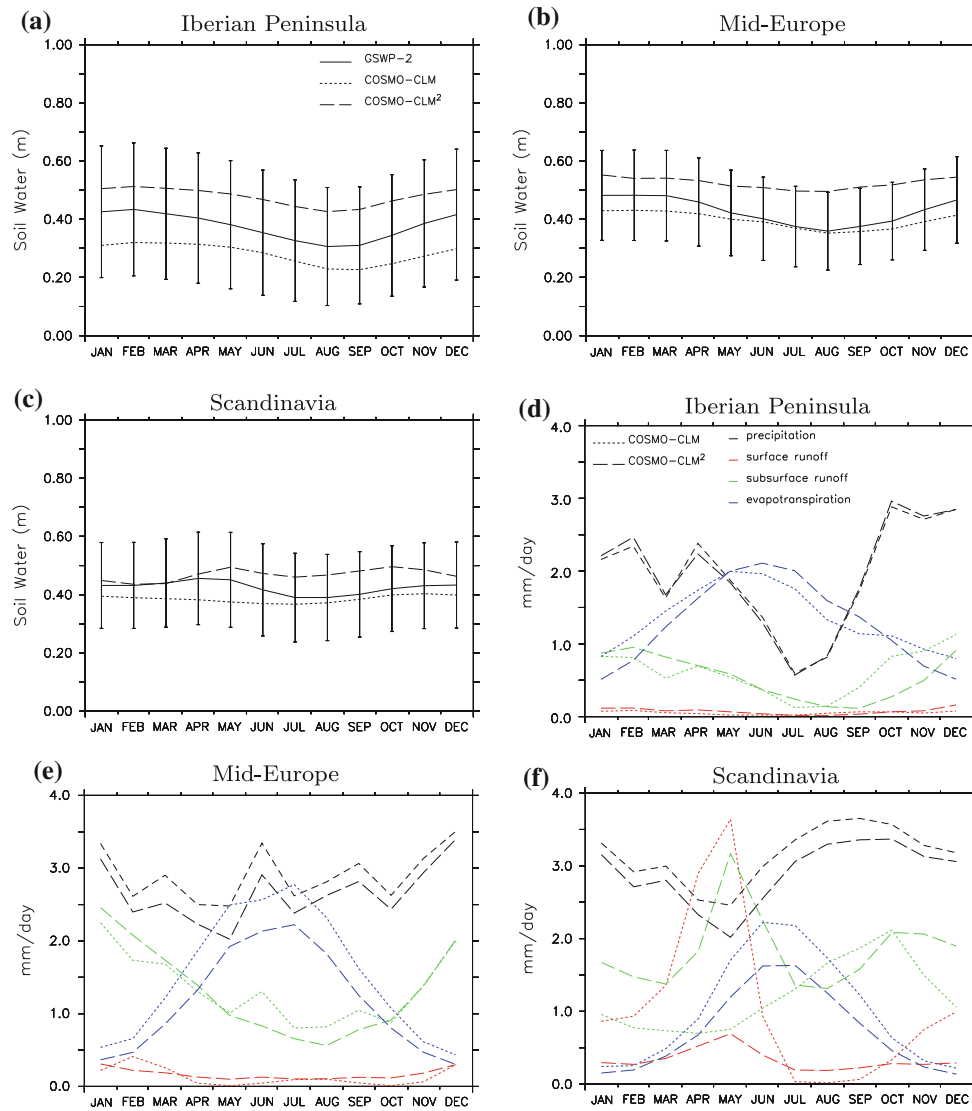


**Fig. 8** a–c Mean seasonal cycle of integrated soil water content between 0 and 1.5 m depth for GSWP-2 (plain line), COSMO-CLM (dotted line) and COSMO-CLM<sup>2</sup> (dashed line). d–f Mean seasonal cycle of precipitation (black), evapotranspiration (blue), surface (red)

and subsurface (green) runoff for COSMO-CLM (dotted line) and COSMO-CLM<sup>2</sup> (dashed line). Climatological means are calculated over the period 1986–1995

### 3.5 Interannual variability

Beside the mean climate state we also examine the model ability to reproduce observed interannual variability. We consider year-to-year anomalies in summer (JJA) 2-meter temperature for the period 1986–2006. Table 5 indicates correlation coefficients between observed and modeled time series for eight different regions.

Overall, observed interannual variations in temperature are well reproduced by both model versions, with correlations ranging from 0.67 to 0.98. These relatively good correlations can be attributed in the first place to the use of reanalysis data for SSTs and lateral boundary conditions,

which already contain the large-scale features of interannual variability. However, the more detailed regional features (e.g., local magnitude of anomalies) are affected by local feedback processes, which directly reflect model skills. In this respect, COSMO-CLM<sup>2</sup> systematically exhibits higher correlations than COSMO-CLM for all regions, indicating a better representation of these local feedback processes. The largest improvements are seen for Eastern Europe and the Mediterranean where the correlations with observations increased from 0.67 to 0.88 and from 0.75 to 0.88, respectively. We note however no clear improvement in the simulated interannual variability for precipitation (not shown).

**Table 5** Performance of the 2 model versions in simulating inter-annual summer variability (JJA average) for 2-m temperature

| Domain            | COSMO-CLM | COSMO-CLM <sup>2</sup> |
|-------------------|-----------|------------------------|
| British Isles     | 0.97      | 0.98                   |
| Iberian Peninsula | 0.89      | 0.92                   |
| France            | 0.86      | 0.91                   |
| Mid-Europe        | 0.92      | 0.94                   |
| Scandinavia       | 0.93      | 0.94                   |
| Alps              | 0.91      | 0.92                   |
| Mediterranean     | 0.75      | 0.88                   |
| Eastern Europe    | 0.67      | 0.88                   |

Correlation coefficients are calculated in reference to the CRU dataset over the period 1986–2006

#### 4 Discussion

By incorporating a more comprehensive LSM into COSMO-CLM, we find systematic improvements in several aspects of the simulated European climate. In the following discussion we attempt to unravel the physical mechanisms explaining these improvements.

Since only the land surface component is changed between the 2 experiments, the differences in the simulated climate necessarily originate from differing surface fluxes. Analyzing surface fluxes in COSMO-CLM<sup>2</sup> compared to COSMO-CLM, we noted in previous sections: (1) an improved surface radiation budget (reduction of shortwave underestimation) and (2) a better partitioning of turbulent fluxes (higher  $B$ ). The first effect is due to a change in cloud cover (Sect. 3.2) and is thus only an indirect consequence of using a different LSM. Therefore, we hypothesise that the change in  $B$  is the primary factor triggering further improvements of the simulated climate.

The proposed mechanism is illustrated in Fig. 9. As seen in Sect. 3.3,  $B$  is generally higher in COSMO-CLM<sup>2</sup> compared to COSMO-CLM (more sensible heat and less latent heat). This leads to a decrease in cloud cover (and subsequently in precipitation) in two ways. First, reduced latent heat flux implies an overall decrease of the atmospheric water content, consistent with a decrease in the amount of clouds. Second, increased sensible heating produces a warming of the lower part of the troposphere. Because warmer air can contain more water vapor, it allows less cloud condensation to occur. The change in cloud cover in the model is confined to the lower part of the troposphere (not shown), which is in line with this interpretation. Another effect of the decreased moisture flux is a possible increase of the boundary layer height, which acts to further enhance the atmospheric drying (e.g., Eltahir 1998; Schar et al. 1999; Jaeger and Seneviratne in press). Moreover, we note that this physical response is consistent with a positive soil moisture-precipitation feedback in the

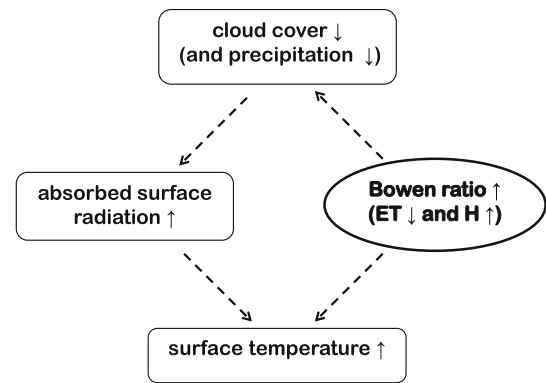


**Fig. 9** Idealized representation of the mechanism leading to the different climate state in COSMO-CLM<sup>2</sup> compared to COSMO-CLM. *Small upward arrows* express an increase, while *small downward arrows* express a decrease. *ET* evapotranspiration; *H* sensible heat

model, as also reported in several other modelling studies with a few exceptions (see e.g. Seneviratne et al. 2010, for a review).

As a consequence of the reduced cloud cover, incoming solar radiation at the surface is enhanced, which has a warming effect on surface temperature. In addition, the higher  $B$  in COSMO-CLM<sup>2</sup> has a direct effect on near-surface temperature, which also corresponds to a warming resulting from enhanced sensible heating at the surface.

In order to test the validity of this hypothesis we perform an additional experiment using COSMO-CLM. Assuming that the better partitioning of turbulent fluxes is the main cause for the better performances of COSMO-CLM<sup>2</sup>, it should be possible to reproduce COSMO-CLM<sup>2</sup> results by tuning  $B$  in COSMO-CLM. As a means of increasing  $B$  in COSMO-CLM, we choose to increase the minimum stomatal resistance ( $r_{s,min}$ ) involved in the calculation of transpiration. By increasing this resistance we expect a limitation of ET and thus an increase in sensible heat (increase in  $B$ ).  $r_{s,min}$  is spatially and temporally constant in TERRA\_ML and set to a default value of 150 s/m. We perform a simulation referred to as COSMO-CLM\_rs300 with the same set up as our COSMO-CLM experiment, except for the value of  $r_{s,min}$  which is set to 300 s/m.

The results of COSMO-CLM\_rs300 compared to COSMO-CLM are shown in Fig. 10. As expected,  $B$  is increased over the whole domain as a consequence of increasing  $r_{s,min}$ . More interestingly, we find that cloud cover, radiation and surface temperature are sensitive to this increase in  $B$ , in a way which is consistent with the general mechanism depicted in Fig. 9 (i.e., a decrease in cloud cover and an increase in absorbed shortwave radiation and in temperature). We note however that the magnitude of the changes in  $B$  and temperature in Fig. 10 remains small in comparison with the COSMO-CLM

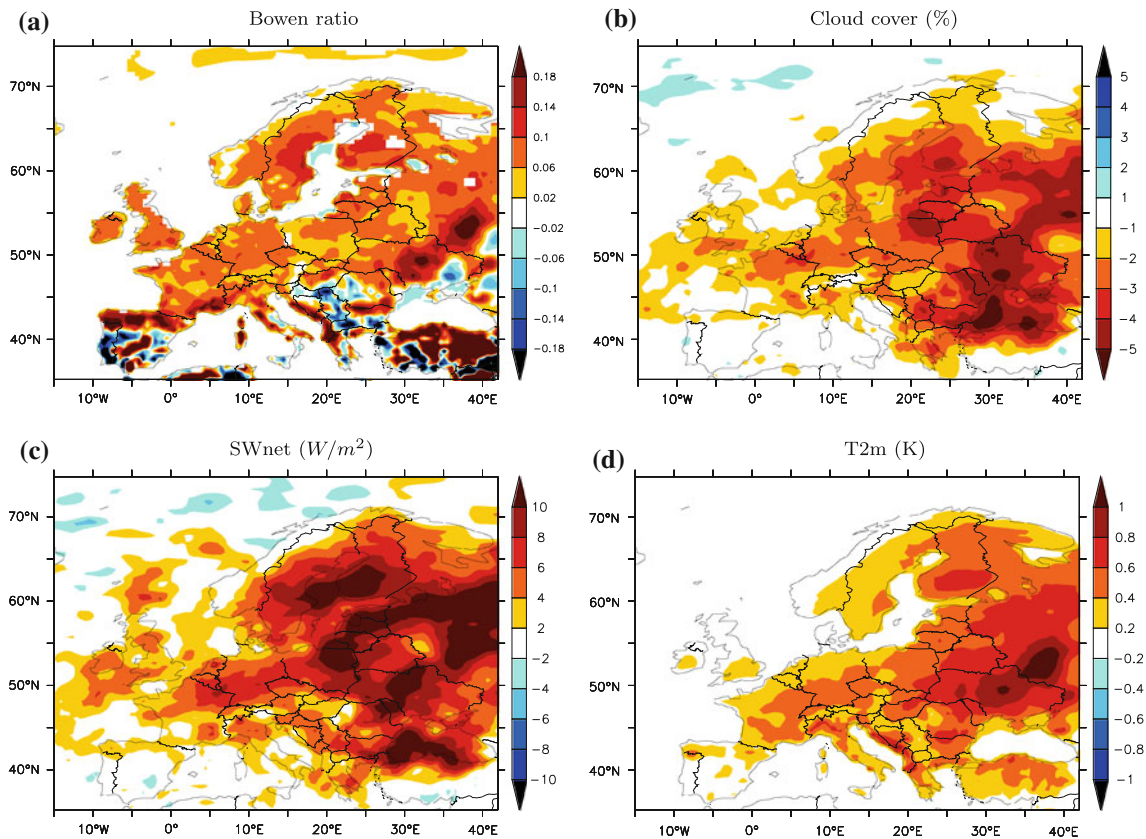


**Fig. 10** Difference between COSMO-CLM\_rs300 and COSMO-CLM (JJA average) for **a** Bowen ratio, **b** cloud cover, **c** surface net shortwave radiation and **d** 2-m temperature

model biases for these quantities (see e.g., Fig. 1c). In other words, our tuning of  $B$  improves COSMO-CLM performances more qualitatively than quantitatively. Nonetheless, this sensitivity experiment confirms the central role of turbulent fluxes partitioning in the context of climate simulations.

We performed additional sensitivity tests with COSMO-CLM by tuning other land surface parameters. For instance, increasing soil resistance or decreasing LAI when calculating evapotranspiration also increases  $B$ , with similar consequences as in the experiment COSMO-CLM\_rs300 described above. However, the overall effect of these parameters remains also relatively small. It is therefore unlikely that COSMO-CLM<sup>2</sup> performances can be quantitatively reproduced just by tuning COSMO-CLM parameters. This suggests that structural differences between the two models may play a major role in explaining the different partitioning of surface fluxes. One important structural difference relates to the more detailed representation of the canopy layer in CLM3.5. CLM3.5 calculates a separate energy balance for the soil and the canopy resulting in distinct temperatures for the vegetation and the soil surface. Fluxes of sensible heat and latent heat are then derived both for canopy and soil

using the respective temperatures. Although there are no straightforward ways to isolate the effect of this representation versus the use of a single bulk surface temperature and energy balance as in TERRA\_ML, it is expected that this may cause important differences in the simulated fluxes.

## 5 Conclusions

The coupling we implemented reemphasizes the importance of land surface processes for the European climate (e.g., Seneviratne et al. 2010; Zampieri et al. 2009; Teuling et al. 2010). Indeed, by changing only the land surface parameterization in COSMO-CLM, we find very substantial differences in the simulated climate, including surface fluxes, cloud cover, precipitation and temperature. We find a more pronounced effect of the coupling during summer, indicating that land surface processes have a more prominent influence on the atmosphere during this season, which is in line with previous modeling studies (e.g., Koster and Suarez 1995).

Second, incorporating a more comprehensive LSM into COSMO-CLM clearly improves the characteristics of the

simulated climate. We find very substantial improvements with respect to land surface fluxes, including an improved magnitude of radiation fluxes and a better partitioning of turbulent fluxes. Furthermore, the model performances for temperature, precipitation and cloud cover are also improved. Given the numerous differences between the two model versions regarding land surface representation, several aspects can be relevant for the overall behaviour of the respective model versions. However, based on an additional sensitivity experiment, we conclude that the better partitioning of turbulent fluxes can be seen as the main cause for the improved performances of COSMO-CLM<sup>2</sup> over COSMO-CLM.

It should be noted that the version of COSMO-CLM used in this study has some large biases. The coupling with CLM3.5 has a positive influence by reducing these biases, but some significant deficiencies still remain, such as an underestimation of surface net shortwave radiation. Moreover, future work should further investigate if the beneficial effect of the new LSM is robust across different versions of COSMO-CLM. In particular, new developments in the atmospheric scheme have been recently implemented (such as a revised implementation of the Tiedtke scheme and an improved time filtering of the leapfrog scheme) and preliminary results indicate a clear reduction of the model biases due to these modifications (D. Luethi, personal communication). Research is currently underway to evaluate whether the coupling with CLM3.5 is also beneficial in the context of this new version.

**Acknowledgments** We are grateful to Daniel Luethi for his technical help regarding the simulation setup. We appreciated the valuable comments from Juergen Helmert and Hermann Asensio concerning TERRA\_ML. We would like to thank the following FLUXNET PIs for providing access to their data: Michael Marek (CZBK1), Riccardo Valentini (ITamp), André Granier (FRHes), Timo Vesala (FIHy), Tuomas Laurila (FIKaa, FISod), Serge Rambal (FRPue), Stefano Minerbi (ITRen), Marc Aubinet (BEVie), and Martin Heimann (RUFyo). We also acknowledge the use of ferret and R for plots. The computing time was provided by the Swiss National Supercomputing Centre (CSCS). This research has been supported by the Competence Center Environment and Sustainability of the ETH Domain (CCES) through the MAIOLICA project. The National Center for Atmospheric Research is sponsored by the US National Science Foundation.

## References

- Adler R, Huffman G, Chang A, Ferraro R, Xie P, Janowiak J, Rudolf B, Schneider U, Curtis S, Bolvin D, Gruber A, Susskind J, Arkin P, Nelkin E (2003) The version-2 global precipitation climatology project (GPCP) monthly precipitation analysis (1979–present). *J Hydrometeorol* 4(6):1147–1167
- Anders I, Rockel B (2009) The influence of prescribed soil type distribution on the representation of present climate in a regional climate model. *Clim Dyn* 33(2–3):177–186. doi:10.1007/s00382-008-0470-y
- Arneth A, Harrison SP, Zaehle S, Tsigaridis K, Menon S, Bartlein PJ, Feichter J, Korhola A, Kulmala M, O'Donnell D, Schurgers G, Sorvari S, Vesala T (2010) Terrestrial biogeochemical feedbacks in the climate system. *Nat Geosci* 3(8):525–532. doi:10.1038/ngeo905
- Aubinet M, Chermaine B, Vandenhaute M, Longdoz B, Yernaux M, Laitat E (2001) Long term carbon dioxide exchange above a mixed forest in the Belgian Ardennes. *Agric For Meteorol* 108(4):293–315
- Avissar R, Pielke R (1989) A parameterization of heterogeneous land surfaces for atmospheric numerical-models and its impact on regional meteorology. *Mon Weather Rev* 117(10):2113–2136
- Avissar R, Pielke R (1991) The impact of plant stomatal control on mesoscale atmospheric circulations. *Agric For Meteorol* 54(2–4):353–372
- Baldocchi D, Falge E, Gu LH, Olson R, Hollinger D, Running S, Anthoni P, Bernhofer C, Davis K, Evans R, Fuentes J, Goldstein A, Katul G, Law B, Lee XH, Malhi Y, Meyers T, Munger W, Oechel W, Paw U KT, Pilegaard K, Schmid HP, Valentini R, Verma S, Vesala T, Wilson K, Wofsy S (2001) FLUXNET: A new tool to study the temporal and spatial variability of ecosystem-scale carbon dioxide, water vapor, and energy flux densities. *Bull Am Meteorol Soc* 82(11):2415–2434
- Beven KJ, Kirkby MJ, Schofield N, Tagg AF (1984) Testing a physically based flood forecasting model (TOPMODEL) for 3 UK catchments. *J Hydrol* 69(1–4):119–143
- Bonan GB (2008) Forests and climate change: forcings, feedbacks, and the climate benefits of forests. *Sci Agric* 320(5882):1444–1449. doi:10.1126/science.1155121
- Bonan G, Levis S (2006) Evaluating aspects of the community land and atmosphere models (CLM3 and CAM3) using a dynamic global vegetation model. *J Clim* 19(11):2290–2301
- Bonan G, Levis S, Kergoat L, Oleson K (2002) Landscapes as patches of plant functional types: An integrating concept for climate and ecosystem models. *Glob Biogeochem Cycles* 16(2):1021. doi:10.1029/2000GB001360
- Christensen JH, Hewitson B, Busuioc A, Chen A, Gao X, Held I, Jones R, Kolli RK, Kwon WT, Laprise R, Magaña Rueda V, Mearns L, Menéndez CG, Ráisiänen J, Rinke A, Sarr A, Whetton P (2007a) Regional climate projections. In: Solomon S, Qin D, Manning M, Chen Z, Marquis M, Averyt KB, Tignor M, Miller HL (eds) *Climate change 2007: the physical science basis. Contribution of working group I to the 4th assessment report of the intergovernmental panel on climate change*. Cambridge University Press, Cambridge
- Christensen JH, Carter TR, Rummukainen M, Amanatidis G (2007b) Evaluating the performance and utility of regional climate models: the PRUDENCE project. *Clim Change* 81(Suppl. 1):1–6. doi:10.1007/s10584-006-9211-6
- Christensen JH, Boberg F, Christensen OB, Lucas-Picher P (2008) On the need for bias correction of regional climate change projections of temperature and precipitation. *Geophys Res Lett* 35(20):L20709. doi:10.1029/2008GL035694
- Collatz GJ, Ball JT, Grivet C, Berry JA (1991) Physiological and environmental regulation of stomatal conductance, photosynthesis and transpiration—a model that includes a laminar boundary layer. *Agric For Meteorol* 54(2–4):107–136
- Collatz GJ, Ribas-Carbo M, Berry JA (1992) Coupled photosynthesis-stomatal conductance model of leaves for C<sub>4</sub> plants. *Aust J Plant Physiol* 19:519–538
- Collins WD, Bitz CM, Blackmon ML, Bonan GB, Bretherton CS, Carton JA, Chang P, Doney SC, Hack JJ, Henderson TB, Kiehl JT, Large WG, McKenna DS, Santer BD, Smith RD (2006) The community climate system model version 3 (CCSM3). *J Clim* 19(11):2122–2143

- Denning A, Nicholls M, Prihodko L, Baker I, Vidale P, Davis K, Bakwin P (2003) Simulated variations in atmospheric CO<sub>2</sub> over a Wisconsin forest using a coupled ecosystem-atmosphere model. *Glob Change Biol* 9(9):1241–1250
- Dickinson RE (1984) Modelling evapotranspiration for three-dimensional global climate models. In: Hansen J, Takahashi T (eds) *Geophysical Monograph 29, Maurice Ewing vol 5, Climate processes and climate sensitivity*. American Geophysical Union, Washington, pp 58–72
- Dickinson R, Oleson K, Bonan G, Hoffman F, Thornton P, Vertenstein M, Yang Z, Zeng X (2006) The Community Land Model and its climate statistics as a component of the Community Climate System Model. *J Clim* 19(11):2302–2324
- Dirmeyer PA, Gao X, Zhao M, Guo Z, Oki T, Hanasaki N (2006) GSWP-2—Multimodel analysis and implications for our perception of the land surface. *Bull Am Meteorol Soc* 87(10):1381. doi: [10.1175/BAMS-87-10-1381](https://doi.org/10.1175/BAMS-87-10-1381)
- Dougherty RL, Bradford JA, Coyne PI, Sims PL (1994) Applying an empirical model of stomatal conductance to 3 C<sub>4</sub> grasses. *Agric For Meteorol* 67(3–4):269–290
- Eltahir E (1998) A soil moisture rainfall feedback mechanism 1. Theory and observations. *Water Resour Res* 34(4):765–776
- Farquhar GD, von Caemmerer S, Berry JA (1980) A biochemical model of photosynthesis CO<sub>2</sub> fixation in leaves of C<sub>3</sub> species. *Planta Med* 149:78–90
- Gilmanov TG, Soussana JE, Aires L, Allard V, Ammann C, Balzarolo M, Barcza Z, Bernhofer C, Campbell CL, Cernusca A, Cescatti A, Clifton-Brown J, Dirks BOM, Dore S, Eugster W, Fuhrer J, Gimeno C, Gruenwald T, Haszpra L, Hensen A, Ibrom A, Jacobs AFG, Jones MB, Lanigan G, Laurila T, Lohila A, Manca G, Marcolla B, Nagy Z, Pilegaard K, Pinter K, Pio C, Raschi A, Rogiers N, Sanz MJ, Stefani P, Sutton M, Tuba Z, Valentini R, Williams ML, Wohlfahrt G (2007) Partitioning European grassland net ecosystem CO<sub>2</sub> exchange into gross primary productivity and ecosystem respiration using light response function analysis. *Agric Ecosyst Environ* 121(1–2):93–120. doi: [10.1016/j.agee.2006.12.008](https://doi.org/10.1016/j.agee.2006.12.008)
- Giorgi F (2006) Regional climate modeling: status and perspectives. *J Phys IV* 139:101–118. doi: [10.1051/jp4:2006139008](https://doi.org/10.1051/jp4:2006139008)
- Granier A, Ceschia E, Damesin C, Dufrene E, Epron D, Gross P, Lebaube S, Le Dantec V, Le Goff N, Lemoine D, Lucot E, Ottorini J, Pontailler J, Saugier B (2000) The carbon balance of a young Beech forest. *Funct Ecol* 14(3):312–325
- Grasselt R, Schuettmeyer D, Warrach-Sagi K, Ament F, Simmer C (2008) Validation of TERRA-ML with discharge measurements. *Meteorol Z* 17(6, Sp. Iss. SI):763–773. doi: [10.1127/0941-2948/2008/0334](https://doi.org/10.1127/0941-2948/2008/0334)
- Hatakka J, Aalto T, Aaltonen V, Aurela M, Hakola H, Komppula M, Laurila T, Lihavainen H, Paatero J, Salminen K, Viisanen Y (2003) Overview of the atmospheric research activities and results at Pallas GAW station. *Boreal Environ Res* 8(4):365–383
- Heald CL, Henze DK, Horowitz LW, Feddes J, Lamarque JF, Guenther A, Hess PG, Vitt F, Seinfeld JH, Goldstein AH, Fung I (2008) Predicted change in global secondary organic aerosol concentrations in response to future climate, emissions, and land use change. *J Geophys Res* 113(D5):D05211. doi: [10.1029/2007JD009092](https://doi.org/10.1029/2007JD009092)
- Hillel D (1980) *Applications of soil physics*. Academic Press, New York
- Hirschi M, Viterbo P, Seneviratne SI (2006) Basin-scale water-balance estimates of terrestrial water storage variations from ECMWF operational forecast analysis. *Geophys Res Lett* 33(21):L21401. doi: [10.1029/2006GL027659](https://doi.org/10.1029/2006GL027659)
- Hohenegger C, Brockhaus P, Bretherton CS, Schaer C (2009) The soil moisture-precipitation feedback in simulations with explicit and parameterized convection. *J Clim* 22(19):5003–5020. doi: [10.1175/2009JCLI2604.1](https://doi.org/10.1175/2009JCLI2604.1)
- Jacob D, Barring L, Christensen OB, Christensen JH, de Castro M, Deque M, Giorgi F, Hagemann S, Lenderink G, Rockel B, Sanchez E, Schaer C, Seneviratne SI, Somot S, van Ulden A, van den Hurk B (2007) An inter-comparison of regional climate models for Europe: model performance in present-day climate. *Clim Change* 81(Suppl. 1):31–52. doi: [10.1007/s10584-006-9213-4](https://doi.org/10.1007/s10584-006-9213-4)
- Jaeger EB, Seneviratne SI (in press) Impact of soil moisture-atmosphere coupling on European climate extremes and trends in a regional climate model. *Clim Dyn*
- Jaeger EB, Anders I, Luethi D, Rockel B, Schaer C, Seneviratne SI (2008) Analysis of ERA40-driven CLM simulations for Europe. *Meteorol Z* 17(4, Sp. Iss. SI):349–367. doi: [10.1127/0941-2948/2008/0301](https://doi.org/10.1127/0941-2948/2008/0301)
- Jaeger EB, Stoeckli R, Seneviratne SI (2009) Analysis of planetary boundary layer fluxes and land-atmosphere coupling in the regional climate model CLM. *J Geophys Res* 114:D17106. doi: [10.1029/2008JD011658](https://doi.org/10.1029/2008JD011658)
- Koster RD, Suarez MJ (1995) Relative contributions of land and ocean processes to precipitation variability. *J Geophys Res* 100(D7):13,775–13,790
- Kothe S, Dobler A, Beck A, Ahrens B (in press) The radiation budget in a regional climate model. *Clim Dyn*
- Kumar SV, Peters-Lidard CD, Eastman JL, Tao WK (2008) An integrated high-resolution hydrometeorological modeling testbed using LIS and WRF. *Environ Model Softw* 23(2):169–181. doi: [10.1016/j.envsoft.2007.05.012](https://doi.org/10.1016/j.envsoft.2007.05.012)
- Laurila T, Soegaard H, Lloyd C, Aurela M, Tuovinen J, Nordstroem C (2001) Seasonal variations of net CO<sub>2</sub> exchange in European Arctic ecosystems. *Theor Appl Climatol* 70(1–4):183–201
- Lawrence PJ, Chase TN (2007) Representing a new MODIS consistent land surface in the Community Land Model (CLM 3.0). *J Geophys Res* 112(G1):G01023. doi: [10.1029/2006JG000168](https://doi.org/10.1029/2006JG000168)
- Levis S, Wiedinmyer C, Bonan G, Guenther A (2003) Simulating biogenic volatile organic compound emissions in the Community Climate System Model. *J Geophys Res* 108(D21):4659. doi: [10.1029/2002JD003203](https://doi.org/10.1029/2002JD003203)
- Lorenz R, Jaeger EB, Seneviratne SI (2010) Persistence of heat waves and its link to soil moisture memory. *Geophys Res Lett* 37:L09703. doi: [10.1029/2010GL042764](https://doi.org/10.1029/2010GL042764)
- Lu L, Pielke R, Liston G, Parton W, Ojima D, Hartman M (2001) Implementation of a two-way interactive atmospheric and ecological model and its application to the central United States. *J Clim* 14(5):900–919
- Marcolla B, Cescatti A, Montagnani L, Manca G, Kerschbaumer G, Minerbi S (2005) Importance of advection in the atmospheric CO<sub>2</sub> exchanges of an alpine forest. *Agric For Meteorol* 130(3–4):193–206. doi: [10.1016/j.agrformet.2005.03.006](https://doi.org/10.1016/j.agrformet.2005.03.006)
- Mellor GL, Yamada T (1974) Hierarchy of turbulence closure models for planetary boundary-layers. *J Atmos Sci* 31(7):1791–1806
- Mellor GL, Yamada T (1982) Development of a turbulence closure-model for geophysical fluid problems. *Rev Geophys* 20(4):851–875
- Milyukova I, Kolle O, Varlagin A, Vygodskaya N, Schulze E, Lloyd J (2002) Carbon balance of a southern taiga spruce stand in European Russia. *Tellus Ser B-Chem Phys Meteorol* 54(5):429–442
- Mitchell T, Jones P (2005) An improved method of constructing a database of monthly climate observations and associated high-resolution grids. *Int J Climatol* 25(6):693–712. doi: [10.1002/joc.1181](https://doi.org/10.1002/joc.1181)
- Mühlbauer A, Lohmann U (2009) Sensitivity studies of aerosol-cloud interactions in mixed-phase orographic precipitation. *J Atmos Sci* 66(9):2517–2538. doi: [10.1175/2009JAS3001.1](https://doi.org/10.1175/2009JAS3001.1)
- Niu G, Yang Z, Dickinson R, Gulden L (2005) A simple TOPMOD-EL-based runoff parameterization (SIMTOP) for use in global

- climate models. *J Geophys Res* 110(D21):D21106. doi:[10.1029/2005JD006111](https://doi.org/10.1029/2005JD006111)
- Niu GY, Yang ZL, Dickinson RE, Gulden LE, Su H (2007) Development of a simple groundwater model for use in climate models and evaluation with Gravity Recovery and Climate Experiment data. *J Geophys Res* 112(D7):D07103. doi:[10.1029/2006JD007522](https://doi.org/10.1029/2006JD007522)
- Oleson KW, Dai Y, Bonan GB, Bosilovich M, Dickinson RE, Dirmeyer P, Hoffman F, Houser P, Levis S, Niu GY, Thornton PE, Vertenstein M, Yang ZL, Zeng X (2004) Technical description of the Community Land Model (CLM). NCAR Tech. Note NCAR/TN-461+STR, Natl. Cent. for Atmos. Res., Boulder
- Oleson KW, Niu GY, Yang ZL, Lawrence DM, Thornton PE, Lawrence PJ, Stoeckli R, Dickinson RE, Bonan GB, Levis S, Dai A, Qian T (2008) Improvements to the Community Land Model and their impact on the hydrological cycle. *J Geophys Res* 113(G1):G01021. doi:[10.1029/2007JG000563](https://doi.org/10.1029/2007JG000563)
- Pielke R, Avissar R, Raupach M, Dolman A, Zeng X, Denning A (1998) Interactions between the atmosphere and terrestrial ecosystems: influence on weather and climate. *Glob Change Biol* 4(5):461–475
- Pitman AJ (2003) The evolution of, and revolution in, land surface schemes designed for climate models. *Int J Climatol* 23(5):479–510
- Reichstein M, Tenhunen J, Rouspard O, Ourcival J, Rambal S, Miglietta F, Peressotti A, Pecchiari M, Tirone G, Valentini R (2002) Severe drought effects on ecosystem CO<sub>2</sub> and H<sub>2</sub>O fluxes at three Mediterranean evergreen sites: revision of current hypotheses?. *Glob Change Biol* 8(10):999–1017
- Reichstein M, Falge E, Baldocchi D, Papale D, Aubinet M, Berbigier P, Bernhofer C, Buchmann N, Gilmanov T, Granier A, Grunwald T, Havrankova K, Ilvesniemi H, Janous D, Knohl A, Laurila T, Lohila A, Loustau D, Matteucci G, Meyers T, Miglietta F, Ourcival J, Pumpanen J, Rambal S, Rotenberg E, Sanz M, Tenhunen J, Seufert G, Vaccari F, Vesala T, Yakir D, Valentini R (2005) On the separation of net ecosystem exchange into assimilation and ecosystem respiration: review and improved algorithm. *Glob Change Biol* 11(9):1424–1439. doi:[10.1111/j.1365-2486.2005.001002.x](https://doi.org/10.1111/j.1365-2486.2005.001002.x)
- Richardson A, Hollinger D, Burba G, Davis K, Flanagan L, Katul G, Munger J, Ricciuto D, Stoy P, Suyker A, Verma S, Wofsy S (2006) A multi-site analysis of random error in tower-based measurements of carbon and energy fluxes. *Agric For Meteorol* 136(1–2):1–18. doi:[10.1016/j.agrformet.2006.01.007](https://doi.org/10.1016/j.agrformet.2006.01.007)
- Ritter B, Geleyn J (1992) A comprehensive radiation scheme for numerical weather prediction models with potential applications in climate simulations. *Mon Weather Rev* 120(2):303–325
- Rockel B, Will A, Hense A (eds) (2008) Special issue: regional climate modelling with COSMO-CLM (CCLM), 4, vol 17. *Meteorol Z*
- Rossow W, Schiffer R (1999) Advances in understanding clouds from ISCCP. *Bull Am Meteorol Soc* 80(11):2261–2287
- Schar C, Luthi D, Beyerle U, Heise E (1999) The soil-precipitation feedback: a process study with a regional climate model. *J Clim* 12(3):722–741
- Sellers PJ, Dickinson RE, Randall DA, Betts AK, Hall FG, Berry JA, Collatz GJ, Denning AS, Mooney HA, Nobre CA, Sato N, Field CB, HendersonSellers A (1997) Modeling the exchanges of energy, water, and carbon between continents and the atmosphere. *Sci Agric* 275(5299):502–509
- Seneviratne SI, Corti T, Davin EL, Hirschi M, Jaeger EB, Lehner I, Orlowsky B, Teuling AJ (2010) Investigating soil moisture-climate interactions in a changing climate: a review. *Earth Sci Rev* 99(3–4):125–161. doi:[10.1016/j.earscirev.2010.02.004](https://doi.org/10.1016/j.earscirev.2010.02.004)
- Smiatek G, Rockel B, Schaettler U (2008) Time invariant data preprocessor for the climate version of the COSMO model (COSMO-CLM). *Meteorol Z* 17(4, Sp. Iss. SI):395–405. doi:[10.1127/0941-2948/2008/0302](https://doi.org/10.1127/0941-2948/2008/0302)
- Steiner A, Pal J, Giorgi F, Dickinson R, Chameides W (2005) The coupling of the Common Land Model (CLM0) to a regional climate model (RegCM). *Theor Appl Climatol* 82(3–4):225–243. doi:[10.1007/s00704-005-0132-5](https://doi.org/10.1007/s00704-005-0132-5)
- Steiner AL, Pal JS, Rauscher SA, Bell JL, Diffenbaugh NS, Boone A, Sloan LC, Giorgi F (2009) Land surface coupling in regional climate simulations of the West African monsoon. *Clim Dyn* 33(6):869–892. doi:[10.1007/s00382-009-0543-6](https://doi.org/10.1007/s00382-009-0543-6)
- Stöckli R, Lawrence DM, Niu GY, Oleson KW, Thornton PE, Yang ZL, Bonan GB, Denning AS, Running SW (2008) Use of FLUXNET in the community land model development. *J Geophys Res* 113(G1):G01025. doi:[10.1029/2007JG000562](https://doi.org/10.1029/2007JG000562)
- Suni T, Rinne J, Reissell A, Altimir N, Keronen P, Rannik U, Dal Maso M, Kulmala M, Vesala T (2003) Long-term measurements of surface fluxes above a Scots pine forest in Hyytiälä, southern Finland, 1996–2001. *Boreal Environ Res* 8(4):287–301
- Teuling AJ, Seneviratne SI, Stoeckli R, Reichstein M, Moors E, Ciais P, Luysaert S, van den Hurk B, Ammann C, Bernhofer C, Dellwik E, Gianelle D, Gielen B, Gruenwald T, Klumpp K, Montagnani L, Moureaux C, Sottocornola M, Wohlfahrt G (2010) Contrasting response of European forest and grassland energy exchange to heatwaves. *Nat Geosci* 3(10):722–727. doi:[10.1038/NGEO950](https://doi.org/10.1038/NGEO950)
- Thornton PE, Zimmermann NE (2007) An improved canopy integration scheme for a land surface model with prognostic canopy structure. *J Clim* 20(15):3902–3923. doi:[10.1175/JCLI4222.1](https://doi.org/10.1175/JCLI4222.1)
- Thornton PE, Lamarque JF, Rosenbloom NA, Mahowald NM (2007) Influence of carbon-nitrogen cycle coupling on land model response to CO<sub>2</sub> fertilization and climate variability. *Glob Biogeochem Cycles* 21(4):GB4018. doi:[10.1029/2006GB002868](https://doi.org/10.1029/2006GB002868)
- Tiedtke M (1989) A comprehensive mass flux scheme for cumulus parameterization in large-scale models. *Mon Weather Rev* 117(8):1779–1800
- Uppala S, Kallberg P, Simmons A, Andrae U, Bechtold V, Fiorino M, Gibson J, Haseler J, Hernandez A, Kelly G, Li X, Onogi K, Saarinen S, Sokka N, Allan R, Andersson E, Arpe K, Balmaseda M, Beljaars A, VanDe Berg L, Bidlot J, Bormann N, Caires S, Chevallier F, Dethof A, Dragosavac M, Fisher M, Fuentes M, Hagemann S, Holm E, Hoskins B, Isaksen I, Janssen P, Jenne R, McNally A, Mahfouf J, Morcrette J, Rayner N, Saunders R, Simon P, Sterl A, Trenberth K, Untch A, Vasiljevic D, Viterbo P, Woollen J (2005) The ERA-40 re-analysis. *Q J R Meteorol Soc* 131(612, Part B):2961–3012. doi:[10.1256/qj.04.176](https://doi.org/10.1256/qj.04.176)
- Wang JW, Denning AS, Lu L, Baker IT, Corbin KD, Davis KJ (2007) Observations and simulations of synoptic, regional, and local variations in atmospheric CO<sub>2</sub>. *J Geophys Res* 112(D4):D04108. doi:[10.1029/2006JD007410](https://doi.org/10.1029/2006JD007410)
- Zahn M, von Storch H (2010) Decreased frequency of North Atlantic polar lows associated with future climate warming. *Nat Biotechnol* 467(7313):309–312. doi:[10.1038/nature09388](https://doi.org/10.1038/nature09388)
- Zampieri M, D’Andrea F, Vautard R, Ciais P, de Noblet-Ducoudré N, Yiou P (2009) Hot European summers and the role of soil moisture in the propagation of Mediterranean drought. *J Clim* 22(18):4747–4758. doi:[10.1175/2009JCLI2568.1](https://doi.org/10.1175/2009JCLI2568.1)